4
Channel Estimation and Tracking in Massive MIMO Systems

In previous chapter the channel matrix for massive MIMO systems was explored and modeled. Another crucial part of the system design is that the knowledge of channel matrix at BS is essential as shown in our system model from (2.2) to (2.7). Based on the literature review on channel estimation in chapter 2, the existing pilot-based and blind channel estimation methods have adverse effects on performance. This chapter presents a blind channel estimation and tracking method for massive MIMO systems. One of the properties of massive MIMO channel model developed in chapter 3, i.e., temporal correlation between consecutive RBs over time-frequency grid is exploited in this work.

In recent years, with the appearance of the "turbo principle" [Berrou *et al.*, 1993], the architecture of iterative receivers has become popular. In the existing state-of-the-art MIMO-OFDM technology, iterative channel estimation for refining the pilot-based estimates has been advocated in several research papers [Kadrija *et al.*, 2013; Liu and Sezginer, 2012; Du *et al.*, 2009]. These methods are based on the slow variations in the channel over time due to temporal correlation. Using frequent pilot-based estimates, the system keeps on tracking the channel in such methods. However, such works are limited in the literature for massive MIMO systems. Also, the pilot-free tracking of channel in massive MIMO systems and associated issue of signal to interference plus noise ratio (SINR) need more research in contrast to the existing pilot-training based MIMO-OFDM systems. Inter-stream interference among MTs is a bottleneck for pilot-free massive MIMO systems.

In general, the iterative estimation algorithms have two components: the initial estimation and the convergence process. For convergence process to take place, certain limits are required on the input parameters to the estimation algorithm. Therefore, the initial estimation plays a crucial role in such methods. In existing literature, the initial estimate in such methods is obtained by certain operations on the received signal such as eigenvalue decomposition (EVD) and subspace projection. The convergence process employs some error correction techniques like least square projection (LSP) and least reliable layer (LRL).

The proposed method is designed to fulfill two purposes: first, to blindly correct the channel matrix and second, to track the channel matrix over time. The method takes the advantage of inherently available temporal correlation between two consecutive RBs for tracking the channel. The tracking provides the initial estimates for iterative channel estimation in each RB. The convergence process employs log-likelihood ratio (LLR) based detection and error correction code (turbo code) which leads to correction in the channel estimate. Inside the shell of proposed method, the existing well explored techniques like ZF estimator, LLR detection, turbo code, theory of large random matrices, and the iterative estimation of temporally correlated channel are connected to solve the prominent problem—the channel estimation—in massive MIMO systems. The error correction code needs not be necessarily turbo code. Other codes like convolutional code and low density parity check (LDPC) code can also be used.

The computational complexity of any method in massive MIMO systems is a concern due to large dimensions of the system. The usage of ZF estimator—the best linear unbiased estimator

(BLUE) [Kay, 1993]—keeps the computational complexity lower than that of other blind channel estimation methods. Better applicability in terms of lesser limitation on system parameters over the existing state-of-the-art blind channel estimation methods makes this method more useful for a system design. In the same sequence, the impact of several system parameters like number of BS antennas (N), number of active MTs (K), number of symbols in an RB (T), signal to noise ratio (SNR), the correlation between consecutive RBs (α_b), and the iteration count of the algorithm (C) on the performance of the scheme is studied.

4.1 SYSTEM MODEL

The massive MIMO channel comprises of two components as per the equation (2.6): the small scale fading matrix $\mathbf{H}_{lm}$ and the large scale fading matrix $\mathbf{D}_{lm}$. The large scale fading matrix describes the statistics of the channel which varies slowly and can be estimated without significant burden. The variations in statistics of the channel are typically caused by shadow fading due to buildings, foliage, and other structures. However, the small scale fading matrix changes significantly faster with time, frequency, and space in a typical environment. Therefore, the channel estimation in massive MIMO systems is mainly related to this matrix. It is assumed that the statistics of each channel vector are available at corresponding MTs. In non-cooperative settings among cells, the required channel matrix to be estimated is $\mathbf{H}_{ll}$ ($l = m$) and analysis on a single cell is sufficient with considering the inter-cell interference as additional noise.

Following above assumptions, we drop the cell index l for simplicity. The proposed scheme is independent of the spatial signature of the signal. Therefore, the channel model of (3.2) is further simplified by setting $r_{ijc} = 1$, $p_{ijc} = 0$, and $N_c = 1$. To keep the analysis simple and oriented to small scale fading, β_{ijc} is kept as one which can be assumed under power control at MTs to make the channel vectors statistically symmetric. The correlated block fading assumption of channel model (3.2) is maintained. For a practical system, such a channel model is realized by using the orthogonal frequency division multiplexing (OFDM) to convert a wide-band frequency selective channel into blocks of correlated flat channels with a certain overhead of cyclic prefixes. A typical example is the LTE standard. The proposed method is designed to take the advantage of the correlation between consecutive blocks which may exist along both time and frequency. However, to keep the concept simple, the scheme is limited for utilizing the correlation only along time axis.

Now, considering the aforementioned preambles, if T number of symbols (after removing the cyclic prefixes) are communicated from each MT to BS in a given RB with index (t^b, f^b) and the considered wireless cellular massive MIMO system has K active MTs and one BS with N antennas in a cell, the baseband equivalent received matrix then can be written as:

$$\mathbf{Y}(t^b, f^b) = \mathbf{H}(t^b, f^b)\mathbf{X}(t^b, f^b) + \frac{1}{\sqrt{p_u}}\mathbf{W}(t^b, f^b)\ , \tag{4.1}$$

where

- (t^b, f^b) is the index of RB,
- $\mathbf{Y}(t^b, f^b)$ is an $N \times T$ received complex matrix,
- $\mathbf{X}(t^b, f^b)$ is a $K \times T$ transmitted complex user data matrix where the entries of $\mathbf{X}(t^b, f^b)$ come from an M-QAM (64-QAM in current setup) constellation,
- $\mathbf{W}(t^b, f^b)$ is an $N \times T$ complex AWGN matrix with zero mean unit variance i.i.d. entries, and

- $\mathbf{H}(t^b, f^b)$ is an $N \times K$ baseband equivalent complex channel matrix.

The parameter p_u is a measure of common transmit power. Under the considered symmetric channel vectors, p_u can further be interpreted as an uplink SNR. In non-cooperative multi-cell settings, it is reasonable to assume the inter-cell interference as white and Gaussian distributed. Thus, the system model of (4.1) is also applicable to multi-cell settings where p_u becomes the uplink signal to noise plus inter-cell interference ratio. Setting $p_{ijc} = 0$ in (3.2) makes the elements of $\mathbf{H}(t^b, f^b)$ i.i.d across antennas and MTs. Further, the temporal variations are modeled by using Markov process instead of defining a generalized temporal covariance matrix as in channel model of (3.2) so that the analysis for two consecutive RBs is sufficient to draw an insightful conclusion. The correlation between the channel coefficients in RBs with indexes t^b and $t^b + 1$ is defined by α_b such that

$$\mathbf{H}(t^b + 1, f^b) = \alpha_b \mathbf{H}(t^b, f^b) + \sqrt{\{1 - \alpha_b^2\}}\tilde{\mathbf{W}}(t^b, f^b)\,, \tag{4.2}$$

where $\tilde{\mathbf{W}}(t^b, f^b)$ has zero mean unit variance i.i.d. complex Gaussian entries. Further, the matrix $\tilde{\mathbf{W}}(t^b, f^b)$ is independent of $\mathbf{H}(t^b, f^b)$. The correlation value α_b can be written as:

$$\alpha_b = \mathbb{E}\left[h_{ij}^*(t^b + 1, f^b) h_{ij}(t^b, f^b)\right] \tag{4.3}$$
$$\forall\ 1 \leq i \leq N \text{ and } 1 \leq j \leq K.$$

An overview of signal flow is shown in Figure 4.1. A sequence of F^b number of RBs is assigned to each of K MTs over frequency dimension. Each RB comprises of a certain number of OFDM sub-carriers and a certain number of OFDM symbols. Total number of symbols (T) in an RB is equal to the product of the number of OFDM symbols and the number of OFDM sub-carriers. Thus, each MT communicates TF^b number of symbols in the time span of an RB. The user data at each MT are encoded by $1/3$ rate turbo code with the parameters as per LTE standard. The coding runs across all TF^b symbols.

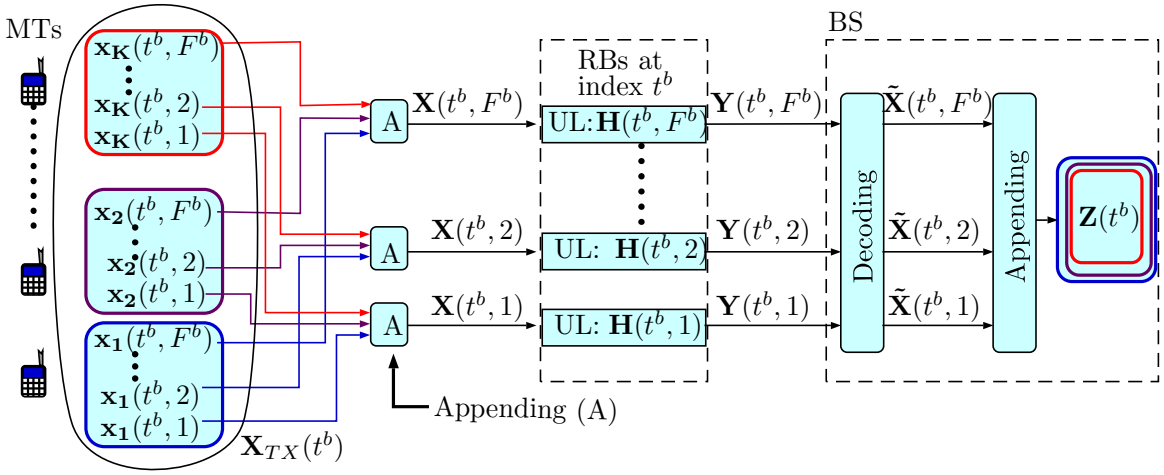

Figure 4.1. : Overview of signal flow

The complete encoded user data matrix from K MTs can be written as:

$$\mathbf{X}_{TX}(t^b) = F_{apn}\left(\mathbf{X}(t^b, 1), \mathbf{X}(t^b, 2), ..., \mathbf{X}(t^b, F^b)\right)\,, \tag{4.4}$$

where F_{apn} represents an operation of horizontal concatenation of matrices. Similarly, the decoded matrix at BS corresponding to K MTs can be written as:

$$\mathbf{Z}(t^b) = F_{apn}\Big(\tilde{\mathbf{X}}(t^b,1), \tilde{\mathbf{X}}(t^b,2), ..., \tilde{\mathbf{X}}(t^b,F^b)\Big). \tag{4.5}$$

The channel matrices are specific to RBs. Therefore, the operation related to channel matrices are performed at block level matrices whereas the encoding and decoding operations are performed at concatenated forms of data.

4.2 CHANNEL ESTIMATION METHOD

The proposed channel estimation algorithm is divided into four sub-sections. First, a few preambles are put in the terms of communication strategy. Next, the algorithm operations are explained step by step. Then, the underlying mathematics is discussed in next sub-section. Finally, an analysis on estimation errors of algorithm is provided.

4.2.1 Communication Strategy and Settings

The proposed algorithm considers a massive MIMO cellular system working in time division duplex (TDD) mode. Under the consideration of temporal correlation from one RB to next RB, the size of RBs is smaller than the coherence time of the channel such that there is a significant correlation between consecutive RBs on time axis. For the first time when communication is initiated, one set of all F^b RBs for $t^b = 1$ comprises of both the uplink data and pilot training symbols which means the channel at $t^b = 1$ is estimated using pilot-based estimation. In subsequent set of F^b RBs (i.e. with $t^b > 1$ and $f^b = 1$ to F^b), MTs send the uplink data encoded over all F^b RBs with T symbols per RB. BS jointly estimates the channel and uplink data. The estimated channel is used to precode the downlink data. BS then transmits the precoded data in same set of RBs in which the uplink data were received. The estimates of channel in current set of RBs (t^b) are passed to next set of RBs ($t^b + 1$) as initial estimates of the channel. The process continues upto completion of the communication. For pilot-based estimation, the MMSE estimation is considered. Same is simulated in this work as follows [Ngo *et al.*, 2013a]:

$$\tilde{\mathbf{H}}_{PBE}(t^b, f^b) = \frac{p_u\tau}{1+p_u\tau}\left\{\mathbf{H}(t^b,f^b) + \frac{1}{\sqrt{p_u\tau}}\mathbf{W}(t^b,f^b)\right\}, \tag{4.6}$$

where τ is the length of uplink pilot train. In order to provide a comparison of proposed scheme with pilot-based scheme, MMSE based estimate of channel is also simulated for each RB separately.

4.2.2 Channel Estimation Algorithm

The flowchart of the the proposed algorithm is shown in Figure 4.2. As per the communication strategy, the algorithm starts with initial estimation of channel using pilot-based estimate received from previous RB. This is indicated by step (1) in the figure. The step (2) is the entry point for the estimate of channel from previous RB during the tracking of channel. In the step (3), an operation of pseudo inverse of the current estimate of channel matrix ($\tilde{\mathbf{H}}(t^b, f^b)$) is performed on the received matrix $\mathbf{Y}(t^b, f^b)$ over all RB indexes from $f^b = 1$ to $f^b = F^b$. Step (4) consists of matrix concatenation function of (4.4) which gives the $K \times TF^b$ dimensional complete encoded user data matrix corresponding to F^b RBs as output. Step (5) uses LLR detecter to generate soft bit outputs corresponding to all K MTs which are further processed by turbo decoder in step (6) to produce error corrected data bits.

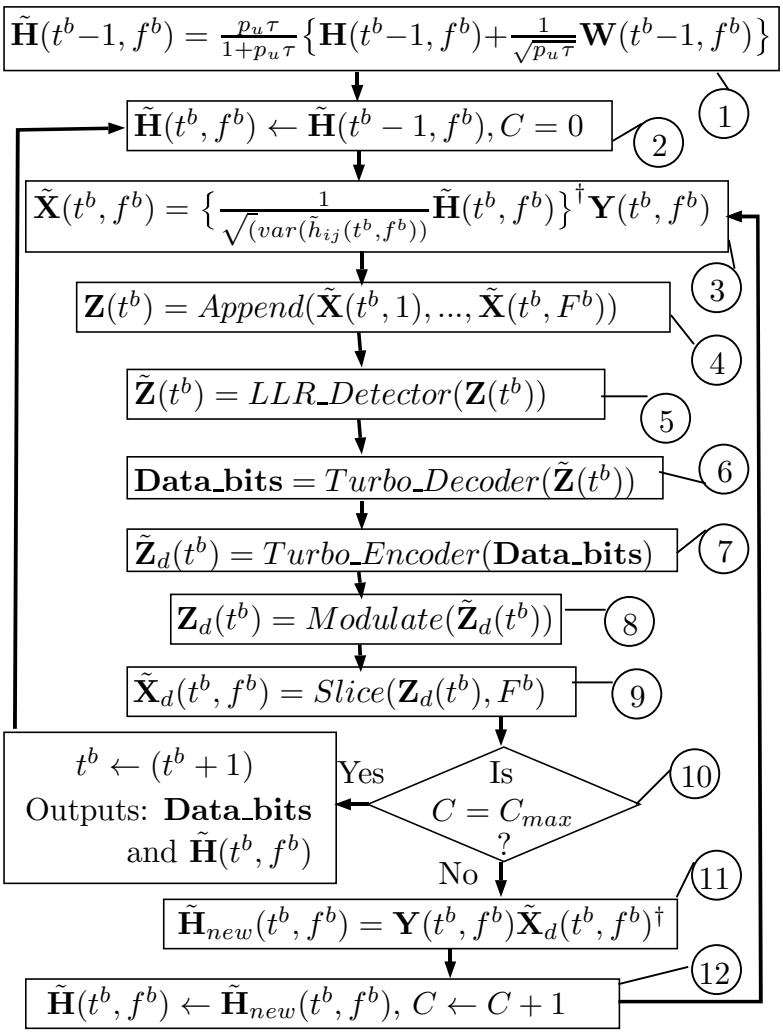

Figure 4.2. : Joint algorithm for channel estimation, data decoding and channel tracking.

The operation of pseudo-inverse in step (3) is the best linear unbiased estimator (BLUE) which performs well under certain limits on N, K, T, α_b, and p_u. This operation of estimation is also justified in the point-of-view of complexity while working with large dimensions. Step (5) and (6) apply the error correction on data bits in each iteration which is basically the essential part of an iterative estimation algorithm. The complexity of LLR detection and max-log-MAP based turbo decoding [Berrou *et al.*, 1993; H. and Wu, 2001] operations in steps (5) and (6) is logarithmic function of constellation size (or linear function of number of bits per constellation point) as they execute on bits in contrast to the existing computationally complex ILSP based algorithm which has complexity exponential in constellation size. The turbo code is one of the best available error correction code. Therefore, the performance improvements over existing blind estimation methods is also significant.

Step (7) applies the turbo encoding on the error corrected bits which are modulated on M-QAM constellation which gives the symbol matrix as output in step (8). Step (9) performs a slicing operation—inverse of append operation of step (4)—on $K \times TF^b$ dimensional symbol matrix to give F^b number of $K \times T$ dimensional matrices as outputs. The iteration count is compared with

a maximum preset value of iteration count in step (10) which takes the decision on terminating or continuing the iterations. While continuing the iterations, step (11) applies the right-sided pseudo-inverse of refined data matrix $\tilde{\mathbf{X}}_d(t^b, f^b)$ on the received matrix $\mathbf{Y}(t^b, f^b)$ for all RBs from $f^b = 1$ to $f^b = F^b$ to produce new refined estimates of channel matrices. Step (12) passes the new estimates to step (3) for next iteration.

A signal flow perspective of proposed algorithm is given in Figure 4.3 for a better understanding. The initial estimates of channel matrices during tracking in step (2) are obtained using the temporal correlation of channel between the RBs with time index t^b and $t^b + 1$. In order to keep the concept simple, the proposed scheme utilizes the simplest way, i.e., to assign the channel estimates of previous set of RBs as initial estimates in current set of RBs. In practice, there are other options for the assignment of initial estimates of the channel matrices. Owing to finite Doppler spectrum of wireless channel [Tse and Viswanath, 2005, Ch 2] and block fading assumption, each channel coefficient—$h_{ij}(t^b, f^b)$—can be considered a band-limited discrete process with time index as t^b. Therefore, the existing extrapolation techniques for band-limited signals [Dharanipragada and Arun, 1997; Shi *et al.*, 2012] can be used to obtain even better initial estimates of the channel matrices while starting the iterations in a new set of RBs.

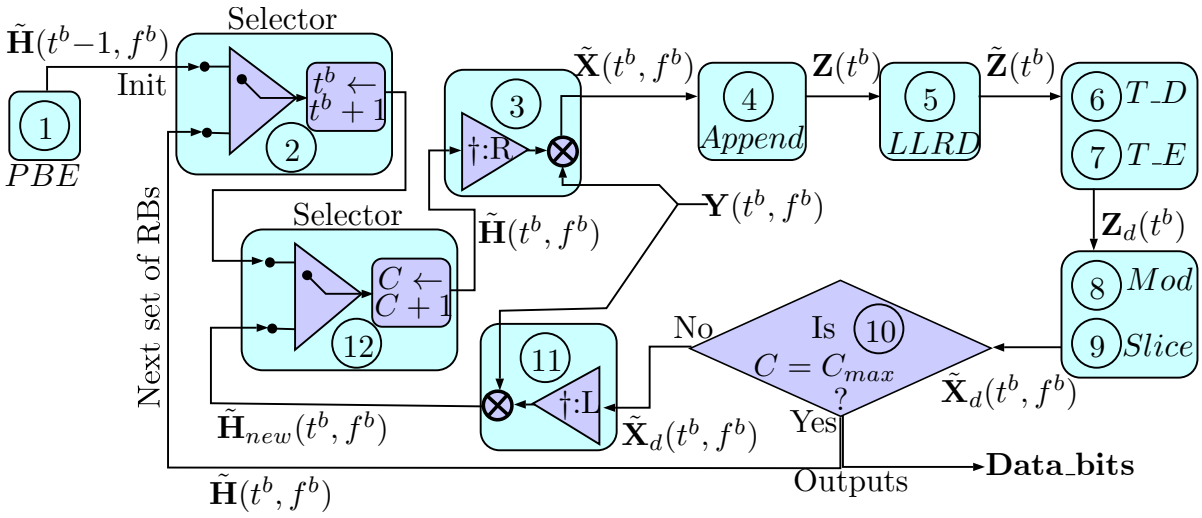

Figure 4.3. : Signal flow prospective of proposed channel tracking algorithm.

4.2.3 Theory Behind the Algorithm

In this subsection, the mathematical basis and the process of convergence for the proposed scheme are provided.

Theorem 4.2.1. *Dropping the indexes t^b and f^b in current system model, i.e.,*

$$\mathbf{Y} = \mathbf{H}\mathbf{X} + \tfrac{1}{\sqrt{p_u}}\mathbf{W},$$

for a given complex valued matrix $\tilde{\mathbf{W}}$ with zero mean unit variance i.i.d. entries and an $\alpha \geq 0$,

$$\lim_{(N\to\infty,\ constant\ K)} \left(\sqrt{1+\alpha^2}\right) \left\{ \frac{(\mathbf{H} + \alpha\tilde{\mathbf{W}})}{\sqrt{1+\alpha^2}} \right\}^{\dagger} \mathbf{Y} = \mathbf{X} \tag{4.7}$$

provided that $\mathbf{H}$ and $\tilde{\mathbf{W}}$ as well as $(\mathbf{H} + \alpha\tilde{\mathbf{W}})$ and $\mathbf{W}$ are independent.

The superscript † is the operation of pseudo inverse. (Proof of theorem 4.2.1: See Annexure A). This theorem reveals the potential of massive MIMO in asymptotic setting which shows that the impact of estimation error in channel can be controlled by changing the dimensions of the system. However, the application of such an operation to the system with finite but large N, T, and small K leads to a finite residual error in the estimate of data matrix. Let the erroneous estimate of data matrix in step (3) of the algorithm (with dropping the indexes t^b and f^b) be

$$\tilde{\mathbf{X}} = \left(\sqrt{1+\alpha^2}\right)\left\{\frac{(\mathbf{H}+\alpha\tilde{\mathbf{W}})}{\sqrt{1+\alpha^2}}\right\}^{\dagger}\mathbf{Y} \tag{4.8}$$

The newly introduced parameter α is a measure of error or deviation in the estimate of channel matrix $\mathbf{H}$. The smaller the α, the better is the estimate of channel matrix. Therefore, α should reduce with iteration count C as per the scheme. For simplicity of the expressions, α is kept free of this index wherever it is out of context. The initial deviation in the estimate of channel matrix (i.e. $\alpha(1)$; $C=1$) arises due to two factors: the accuracy of channel estimate in previous RB and the variations in actual channel matrix from previous RB to current RB. First factor is described by the correlation between the estimate of channel matrix and the actual channel matrix in previous RB (α_e). The second factor is described by the correlation between the true channel elements in previous RB and the true channel elements in current RB (α_b).

$$\alpha_e\alpha_b = \frac{1}{\sqrt{1+\alpha^2(1)}} \tag{4.9}$$

Considering the symmetry of the statistics of channel elements, the α_e and α_b are same for different channel elements. Therefore, they can be defined as follows.

$$\alpha_e = \mathbb{C}orr\Big(h_{ij}(t^b-1,f^b)\ ,\ \tilde{h_{ij}}(t^b-1,f^b)\Big) \tag{4.10}$$

$$\alpha_b = \mathbb{C}orr\Big(h_{ij}(t^b,f^b)\ ,\ h_{ij}(t^b-1,f^b)\Big) \tag{4.11}$$

At the start of communication, the initial estimate in previous RB is obtained by pilot-based estimation. In subsequent RBs, α_e itself increases resulting into better initial estimates under the effect of proposed scheme. Therefore, the first set of RBs when initial estimates of the channel are obtained from pilot-based estimation, is useful for unbiased analysis of estimation error. For this set of RBs,

$$\alpha_e = \mathbb{C}orr\Big(h_{ij}(t^b-1,f^b)\ ,\ \tilde{h_{ij}}(t^b-1,f^b)_{PBE}\Big) \tag{4.12}$$

By using (4.6) and (4.10), α_e for first set of RBs, can be expressed as follows.

$$\alpha_e^2 = \frac{p_u\tau}{1+p_u\tau} \tag{4.13}$$

The estimate $\tilde{\mathbf{X}}$ of data matrix in (4.8) can be approximated by using an empirical study along with the random matrix theory [Tulino and Verdu, 2004] for $N >> K >> 1$ as follows:

$$\tilde{\mathbf{X}} = \mathbf{X} + \left(\sqrt{\frac{\alpha^2(C)K}{N-K}}\right)\mathbf{W}_1 + \left(\sqrt{\frac{1+\alpha^2(C)}{p_u(N-K)}}\right)\mathbf{W}_2 \text{ or} \tag{4.14}$$

$$\tilde{\mathbf{X}} = \mathbf{X} + \Delta\mathbf{X}_A + \Delta\mathbf{X}_B\,, \tag{4.15}$$

where $\Delta\mathbf{X}_A \triangleq \left(\sqrt{\frac{\alpha^2(C)K}{(N-K)}}\right)\mathbf{W}_1$ and $\Delta\mathbf{X}_B \triangleq \left(\sqrt{\frac{1+\alpha^2(C)}{p_u(N-K)}}\right)\mathbf{W}_2$.

$\mathbf{W}_1$ and $\mathbf{W}_2$ are complex AWGN matrices with i.i.d. entries having zero mean and unit variance. In each iteration, the multiplier $\sqrt{1+\alpha^2(C)}$ required in (4.8) is not known where it can be estimated by SNR estimation techniques. LLR in step (5) is calculated for each bit of the each symbol ($\tilde{x}_{ij}$) from each MT [Gallager, 2006]. LLR for b^{th} bit of j^{th} symbol from i^{th} MT is calculated as given in following:

$$L(b,i,j) = log\left[\frac{\sum_{m=1;s_m\in S^0}^{M/2}\left\{e^{-\frac{1}{\sigma^2}|\tilde{x}_{ij}-s_m|^2}\right\}}{\sum_{m=1;s_m\in S^1}^{M/2}\left\{e^{-\frac{1}{\sigma^2}|\tilde{x}_{ij}-s_m|^2}\right\}}\right], \tag{4.16}$$

where S^0 is a subset of constellation points in which the b^{th} bit is zero and S^1 is a subset of constellation points in which the b^{th} bit is one. Parameter σ^2 is the variance of error term $\Delta X_A + \Delta X_B$. LLRs computed for scalar symbols ($\tilde{x}_{ij}$) have performance equivalent to the case if LLRs are computed for symbol vector over time ($[\tilde{\mathbf{x}}^T]_j$) [Gallager, 2006, Th 8.4.1]. LLR-based soft detection is followed by turbo decoding in step (6). The LLR detection and turbo decoding improves the accuracy of estimate $\tilde{\mathbf{X}}$ which leads to better estimates at the output in step (9). Similarly, the new estimate of channel matrix for each frequency block index (f^b) in step (11) can be defined as follows:

$$\tilde{\mathbf{H}}_{new} = \mathbf{Y}\tilde{\mathbf{X}}_d^{\dagger} \text{ or} \tag{4.17}$$

$$\tilde{\mathbf{H}}_{new} = \mathbf{H} + \Delta\mathbf{H}_A + \Delta\mathbf{H}_B. \tag{4.18}$$

The one of the error components in (4.18) is: $\Delta\mathbf{H}_B = \mathbf{W}_4/\sqrt{p_u(T-K)}$. The nature of error components in (4.18) is similar to that of (4.15) as found in simulation study. However, $\Delta\mathbf{H}_A$ does not have an explicit expression in terms of T, K, and p_u yet $\Delta\mathbf{H}_A$ is known to be caused by the error in the estimate $\tilde{\mathbf{X}}_d$ of data matrix.

$\Delta\mathbf{X}_A$ and $\Delta\mathbf{H}_A$ reduce with iteration count due to the improved estimate of channel matrix $\tilde{\mathbf{H}}$ and data matrix $\tilde{\mathbf{X}}_d$ respectively. However, the second error components $\Delta\mathbf{X}_B$ and $\Delta\mathbf{H}_B$ additionally depend on SNR p_u. Therefore, they cannot be minimized just by improving the estimate of channel and data matrices. Rather, they have to be controlled by N, K, and T such that the setting on the system parameters keeps the algorithm in convergeable region. The system parameters N, K, T, p_u, and α_b form a combined boundary. If the system settings reach close to this boundary, the required number of iterations for convergence increases exponentially. On the other hand, slightly inside the boundary, the required number of iterations is very small.

4.2.4 Estimation error analysis

The quantification of the required number of iterations depends on the rate of convergence which further depends on how fast the error components are reducing with iterations. The estimation error in the channel matrix (i.e. E_H) and in data matrix (i.e. E_X) are defined at a given iteration index and block-time index as follows:

$$E_X^2 = \mathbb{E}_{f^b}\left[\frac{1}{KT}\left\|\tilde{\mathbf{X}}(t^b, f^b) - \mathbf{X}(t^b, f^b)\right\|^2\right] \text{ and} \tag{4.19}$$

$$E_H^2 = \mathbb{E}_{f^b}\left[\frac{1}{NK}\left\|\tilde{\mathbf{H}}(t^b, f^b) - \mathbf{H}(t^b, f^b)\right\|^2\right]. \tag{4.20}$$

As discussed in previous subsection, the unbiased analysis of estimation error corresponds to first set of RBs, i.e., at the start of communication when the iteration based algorithm is used for first time where initial estimates of the channel are obtained from pilot-based estimation in previous set of RBs. In the same sequence, Figure 4.4 shows the linearly fitted curve on simulated estimation errors for first set of RBs with blind tracking. The error components in estimated data matrix have more insightful expressions than that of estimated channel matrix while the behaviors of E_X^2 and E_H^2 are similar. Therefore, E_X^2 has been analyzed to quantify the number of iterations required for the algorithm. By using (4.14), E_X^2 can be written as follows:

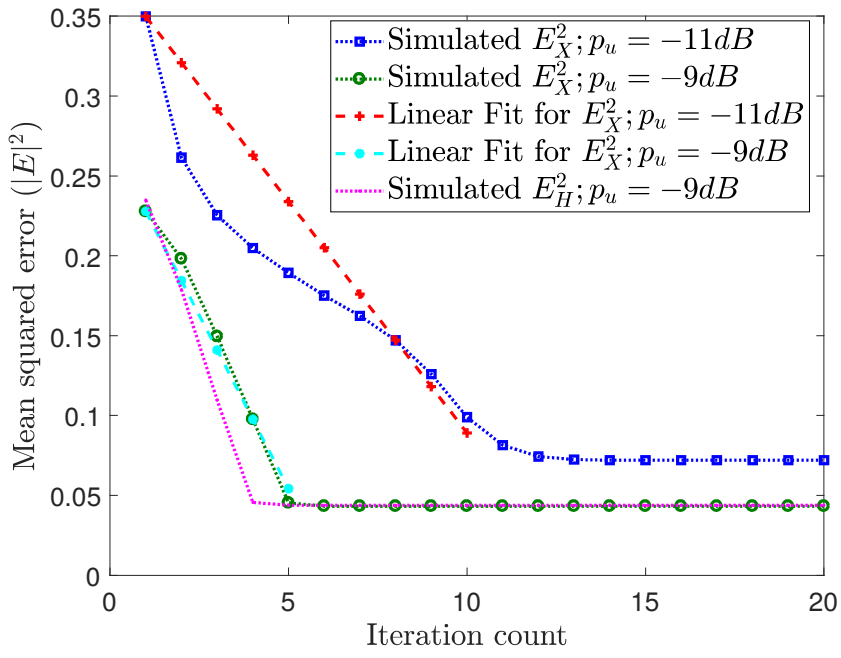

Figure 4.4. : Data and channel estimation error verses iteration counts for different values of p_u (SNR) with $\alpha_b = 0.8$, $K = 20$, $N = 200$ and $T = 200$.

$$E_X^2 = \left(\frac{\alpha^2(C)K}{N-K}\right) + \left(\frac{1+\alpha^2(C)}{p_u(N-K)}\right). \tag{4.21}$$

As shown in Figure 4.4, the change in estimation error with iteration count is not linear. However, the behavior of error with iteration count is less significant. Rather, the number of iterations required for obtaining the final value of estimation error is important. Therefore, a linear fit is used for E_X^2 which can be written as follows:

$$E \overset{(q_1)}{=} E_1 + \frac{E_2 - E_1}{C_2 - C_1}(C - C_1). \tag{4.22}$$

$$\text{At the start, } E_1 \overset{(q_2)}{=} \left(\frac{\alpha^2(1)K}{N-K}\right) + \left(\frac{1+\alpha^2(1)}{p_u(N-K)}\right) \text{ and} \tag{4.23}$$

$$\text{at the end, } E_2 \overset{(q_3)}{=} \left(\frac{\alpha^2(\infty)K}{N-K}\right) + \left(\frac{1+\alpha^2(\infty)}{p_u(N-K)}\right), \tag{4.24}$$

$$\text{where } \alpha^2(\infty) \overset{(q_4)}{=} \frac{1}{p_u(T-K)}. \tag{4.25}$$

q_1 corresponds to linear curve fitting on E_X^2. The initial estimation error (E_1) corresponds to the first iteration count (C_1, i.e., 1) and E_2 is the final estimation error when the convergence completes. q_2 and q_3 follow from the calculation using (4.21) and q_4 follows the calculation of the error component using (4.18) with $\mathbf{\Delta}H_A = 0$.

Next, the least absolute residual (LAR) method is used to fit (4.22) on the simulated mean square error in data matrix versus iteration count as shown in Figure 4.4. With this fitting, the number of iteration counts at the completion of convergence (i.e. C_2) is obtained. An empirical expression for C_2 is established using different values of SNR (p_u), α, and obtained values of C_2 as follows:

$$C_2 = PF\frac{\alpha^2(1) + \alpha^2(\infty)}{p_u}, \tag{4.26}$$

where PF is a proportionality factor which is a measure of capability of error correction code (here turbo code) used in the algorithm. A few values from empirical study are shown in Table 4.1. For current setup, the empirically obtained value of PF is approximately 0.5.

p_u	$\alpha(1)$	$\alpha(\infty)$	C_2	$\frac{\alpha^2(1)+\alpha^2(\infty)}{p_u}$	PF
0.08	1.24	0.26	10.23	20.36	0.50
0.13	1.09	0.21	5.08	9.75	0.52
0.13	1.52	0.21	8.95	18.67	0.48

Table 4.1. : Parameters values (rounded) for establishing empirical expression for C_2 ($\alpha_b = 0.8$, $N = 200$, $K = 20$, and $T = 200$).

4.2.5 Improvement in Spectral Efficiency

The pilot training in proposed scheme is required only at the start of communication. The symbols in subsequent RBs that otherwise are used for training in pilot training based systems, are free for transmission of user data in current scheme as the channel matrices are tracked by incremental updates after each block-time. Therefore, there is an improvement in spectral

efficiency of the system. The spectral efficiency of a multi-user massive MIMO system is given by following [Marzetta, 2010, eq:(14)]:

$$SE = \sum_{k=1}^{K} \left(\frac{B}{\beta}\right) \left(\frac{T_{slot} - T_{pilot}}{T_{slot}}\right) \left(\frac{T_u}{T_{slot}}\right) \log_2\left(1 + SIR_k\right), \tag{4.27}$$

where

- B= total bandwidth,
- β = frequency reuse factor,
- $T_{slot} = T$ = number of symbols in RB,
- $T_{pilot} = K$ = number of pilot symbols in RB,
- SIR_k is signal to interference ratio for k^{th} MT, and
- T_u is the useful OFDM slot.

However, the expression in (4.27) is for MF decoder based system but the pre-log factor, i.e., $(T_{slot} - T_{pilot})/T_{slot}$ is independent of decoder. Using this relation, the proposed scheme provides a gain in spectral efficiency approximately by a factor of $T/(T-K)$ over pilot-based method.

4.3 COMPLEXITY ANALYSIS

The complexity in blind channel estimation methods for massive MIMO systems is an essential concern to be cared of. The complexity of proposed scheme is compared with the existing EVD-ILSP based blind channel estimation method which is closest candidate for comparison in this class. The number of multiplications (and division) are taken as a measure of complexity for comparison. The number of multiplications (plus divisions) per bit in the turbo decoding for a given number of states S and turbo iterations count C_T is given by $8SC_T$ [Chatzigeorgiou *et al.*, 2007, Tab II, Fig 2]. Thus, the number of multiplications in proposed algorithm with C number of iterations can given by following:

$$MUL_{TDC} = 8SC_T C \log_2(M). \tag{4.28}$$

The complexity for one symbol associated with linear operation $\tilde{\mathbf{H}}(t^b, f^b)^\dagger \mathbf{Y}(t^b, f^b)$ is:

$$MUL_{lop1} = \frac{(2NK + K^2 + NT)}{T} C. \tag{4.29}$$

Similarly, the complexity for one symbol associated with linear operation $\mathbf{Y}(t^b, f^b)\tilde{\mathbf{X}}_d(t^b, f^b)^\dagger$ is:

$$MUL_{lop2} = (2K + K^2/T + N)C. \tag{4.30}$$

In the proposed algorithm, the operations corresponding to (4.28), (4.29), and (4.30), are the key contributors to the complexity. Therefore, the total number of multiplications can be approximated as follows:

$$MUL_{IBE} = \left\{(2NK + K^2 + NT)/T + (2K + K^2/T + N) + 8SC_T \log_2(M)\right\} C. \tag{4.31}$$

Next, the complexity of ILSP-based iterative algorithm used in [Ngo and Larsson, 2012] is calculated. This algorithm requires 2^M multiplications where M is the order of modulation. If the use of turbo decoder is considered after the last iteration in this algorithm (for justified comparison), the complexity associated with ILSP-based channel estimation can be written as follows:

$$MUL_{ILSP} = \left\{(2NK + K^2 + NT)/T + (2K + K^2/T + N) + 2^M\right\}C + 8SC_T \log_2(M). \tag{4.32}$$

The ILSP based algorithm in [Ngo and Larsson, 2012] uses the EVD-based blind (almost) method for initial estimation of channel. Therefore, the complexity of EVD-based estimation is also calculated which can be written as follows:

$$MUL_{EVD} = \left\{\frac{N^2}{K} + \frac{N^2}{T} + \frac{NK}{T} + N + K + \frac{8T^2}{K} + \frac{8NT}{K} + \frac{4N}{K} + \frac{4T}{K}\right\}. \tag{4.33}$$

The details regarding the calculation of the number of multiplications for the mathematical operations in 4.33 are provided in Annexure A.

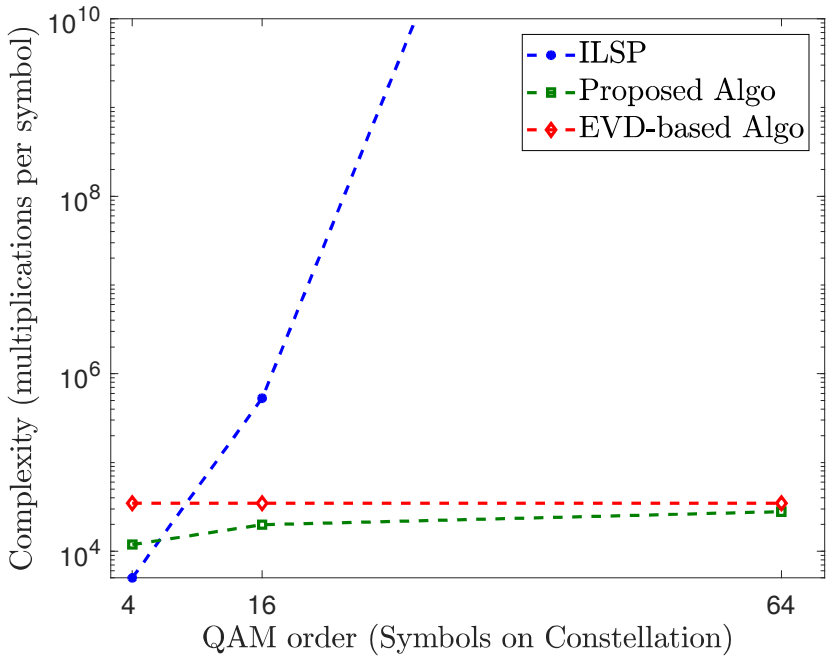

Figure 4.5. : Complexity verses constellation size with $K = 20$, $N = 200$ and $T = 200$.

The comparison of the complexities associated with the proposed algorithm, the EVD-based algorithm, and the ILSP-based algorithm is shown in Figure 4.5. The value of turbo iteration count (C_T) and the number of states in turbo-encoder (S) are 4 and 16 respectively. The value of iteration count (C) in ILSP based and proposed algorithm is 8. The complexity plot shows that the ILSP-based algorithm is not suitable above 4-QAM because complexity increases exponentially. The complexity of proposed algorithm is also lesser than the complexity of EVD-based algorithm.

4.4 SIMULATION RESULTS AND DISCUSSION

The simulation results include the comparison of symbol error probability (SEP) in proposed scheme with that of pilot-based estimation. SEP is regarded same as bit error rate (BER). There is a slight variation in the convention that a bit can be correct or erroneous while a symbol can be partially erroneous depending on the number of erroneous bits in it. Numerically, SEP calculated here is same as BER. The pilot-based estimation is an extensively explored technique in the non-blind class of channel estimation methods. Thus, the comparison of proposed scheme with pilot-based estimation is considered to be useful. However, there are some other methods of blind class as described in chapter 2 which might be considered for comparison but there is a significant variation in the settings on system parameters in these methods from the proposed method. As described in chapter 2, they are mostly dependent on asymptotic settings. The comparison with these schemes is avoided because of their one or some of the specific settings like large N/K ratio (i.e. for better orthogonality of channel vectors), very small size of RB (to keep manageable complexity), large RB (due to dependency on estimated covariance matrix), and smaller size of symbol constellation. Table 4.2 summarizes the settings used in the simulation.

Table 4.2. : Summary of simulation parameters for comparison of pilot-based and proposed iterative channel estimation method.

Parameters	Values	Details
N	100 to 300	Number of BS antennas
K	18 to 24	Number of active MTs
T	150 to 300	Number of symbols in RB
F^b	8 to 15	Number of RBs on frequency axis
T^b	5	Number of RBs considered on time axis
M	64	QAM-order
α_b	0.6 to 0.9	Time correlation in RBs

4.4.1 SEP Verses Iteration Count

This section presents the simulation results in the support of the working of algorithm and the subsection 'Theory behind algorithm' (4.2.3). Figure 4.6 and Figure 4.7 show SEP versus iteration count plots with different values of SNR and channel correlation respectively. When SNR is high (here $-9.5dB$), SEP plot falls quickly with iteration count as shown in Figure 4.6. However, by increasing the iteration count (from 5 to 12 in the figure), the system can support further $2dB$ lower SNR (plot for $p_u = -11.5dB$). As SNR is further lowered, the settings reaches to boundary values which results into the requirement of an exponential increase in iteration counts which is also observed from the plots corresponding to different values of SNR.

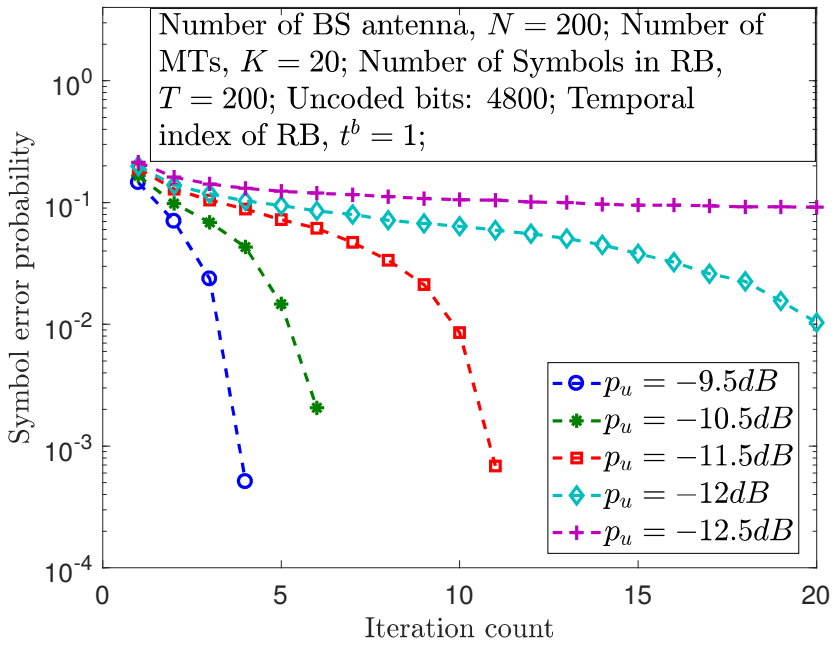

Figure 4.6. : Symbol error probability verses iteration counts for different values of p_u (SNR) with $\alpha_b = 0.8$, $K = 20$, $N = 200$ and $T = 200$.

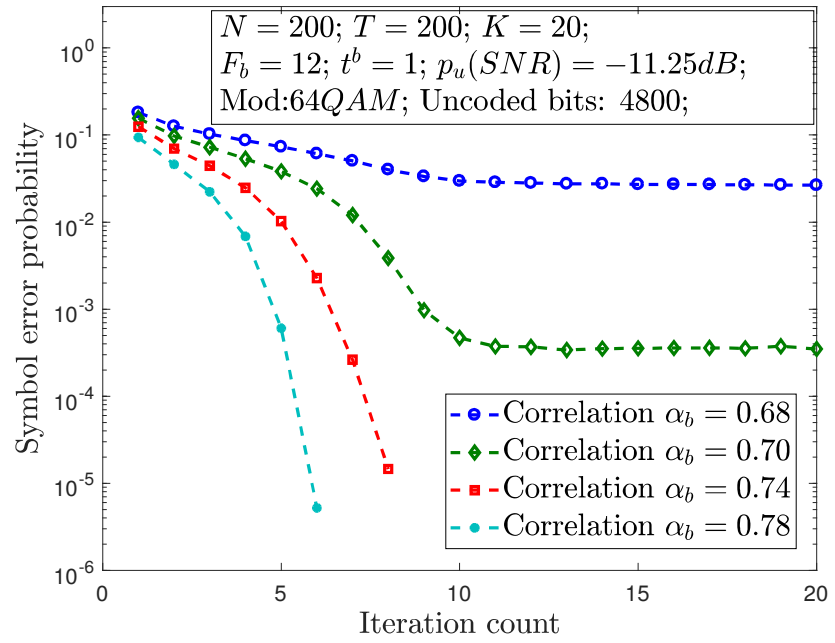

Figure 4.7. : Symbol error probability verses iteration counts for different values of α_b with $p_u = -11.25dB$, $K = 20$, $N = 200$ and $T = 200$.

The ability of the algorithm to deal with different values of temporal correlation between channel elements of consecutive RBs is shown in Figure 4.7. The decreasing correlation can be managed by increasing the iteration counts upto an extent. After that, SEP plot displays an error floor. This difference in the behavior of SEP with channel correlation compared to the behavior of SEP with SNR is caused by the different dependency of error components on SNR and α_b. p_u is connected to second error component in (4.14) while α_b is connected to both of the error components.

To keep the performance comparison unbiased, the first set of RBs, i.e., $t^b = 1 \; \forall \; 1 \leq f^b \leq F^b$ is used for evaluating SEP in proposed scheme where the channel matrices in the previous set of RBs are obtained by pilot-based estimation. The parameter α in analysis comprises of two parameters α_e and α_b where α_e is dependent on the accuracy of channel estimate in previous set of RBs. The settings in which performance of proposed scheme is better than pilot-based estimation, α_e will further reduce for next set of RBs (i.e. $t^b \leftarrow t^b + 1$). After few block times, the steady state is obtained where the performance of proposed scheme is even better. Consequently, the settings on system parameters further can be tightened.

4.4.2 Impact of the Number of MTs

The study on the impact of increasing number of MTs in the system is important because the promise of massive MIMO technology is to provide parallel spatial channels to a large number of MTs in the cells. Against the assumption of infinitely large number of antennas at BS in theory, a practical system must serve the number of MTs as large as possible for a given number of BS antennas and other settings. SEP versus SNR performances of proposed scheme and pilot-based scheme are compared in Figure 4.8 for different number of the active MTs in the cell. The number of iterations in the algorithm is set to 10.

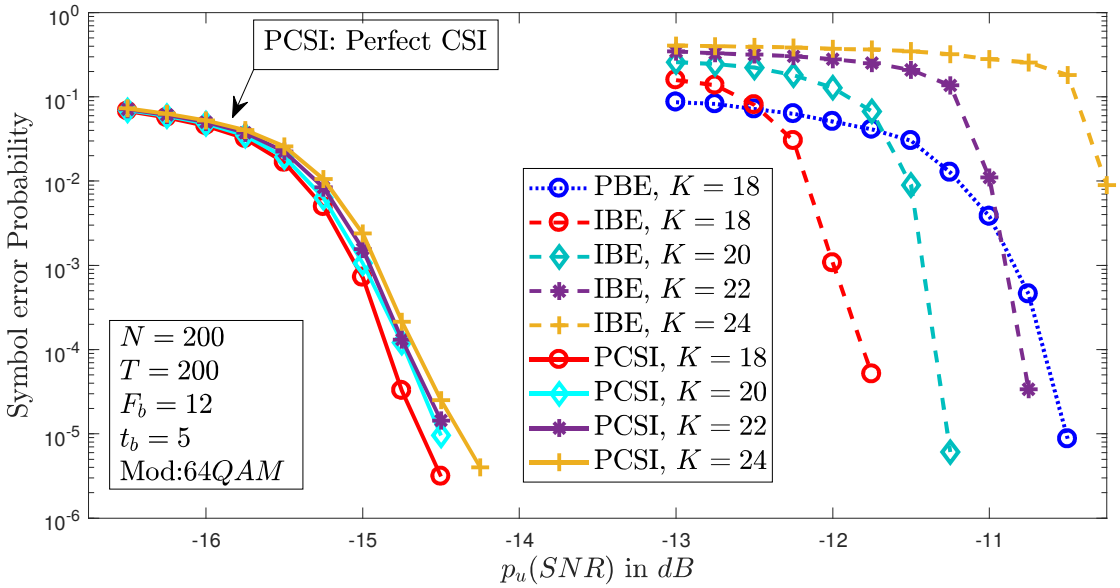

Figure 4.8. : Symbol error probability verses p_u (SNR) for different values of K with $\alpha_b = 0.8$, $N = 200$, $T = 200$ and $t^b = 5$. Right: Proposed algorithm and Left: Capacity limited performance (using ZF with perfect CSI)

SEP in proposed scheme falls significantly earlier than SEP in pilot-based estimation for decreasing number of MTs. The supported ratio of N and K is as small as 10 where the proposed

algorithm performs better than the pilot-based estimation. The impact of the number of BS antennas for a given number of MTs is similar but opposite to the impact of the number of MTs for a given number of BS antennas. This is also supported by the theory as the error expression in 4.14 has N and K coupled together such that they should impose similar but opposite impacts. There is a $3dB$ to $4dB$ SNR margin with respect to the SEP plots for perfect CSI at BS. The impact of number of MTs on the performance of proposed scheme compared to the case of perfect CSI is more because the accuracy of channel estimate varies significantly (cf. sec. (4.2.3)) with number of MTs in the proposed scheme.

4.4.3 Impact of the Mobility

The requirement of the channel matrix and the variations in the channel make the limited coherence time a critical parameter against the performance of massive MIMO systems. The limited coherence time is directly linked to the mobility of MTs. As the coherence time reduces, the correlation between the channels of consecutive RBs reduces which also results into the variations of channel inside the RB. Consequently, the assumptions of time invariant channel inside the RB become difficult to maintain which needs for a reduction in T. In pilot-based estimation, T is directly related to the spectral efficiency of the system. In the blind channel estimation methods, it is directly related to the error performance. The error performance in proposed algorithm is connected to two parameters in this context: α_b and T. Therefore, the study of the impact of mobility includes both α_b and T.

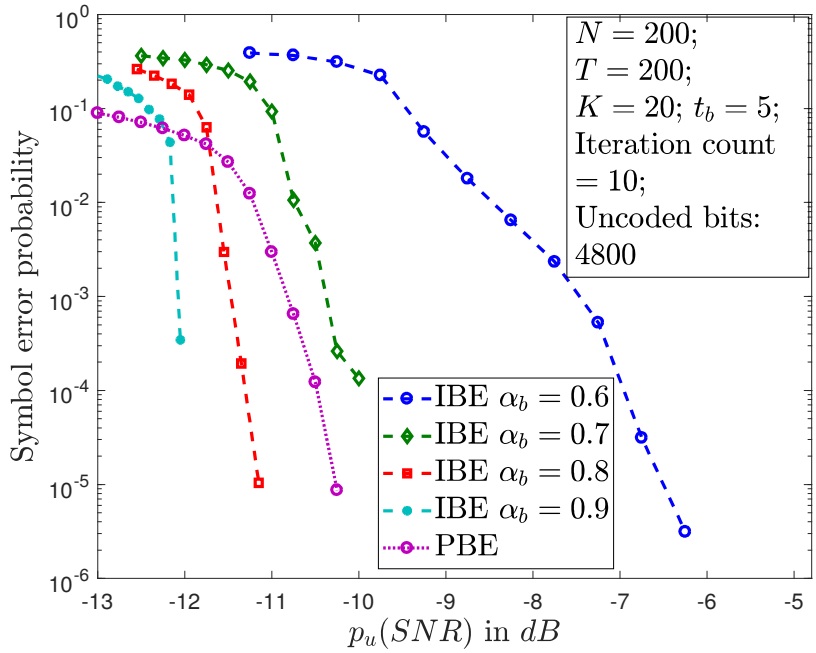

Figure 4.9. : Symbol error probability verses p_u (SNR) for different values of α_b with $K = 20$, $N = 200$, $T = 200$ and $t^b = 5$.

SEP versus SNR performances of the proposed scheme and pilot-based estimation are compared in Figure 4.9 for different values of temporal correlation in the channel of consecutive RBs. The performance of proposed scheme is better than that of pilot-based estimation for temporal correlation values more than approximately 0.75. The smaller value of temporal correlation leads to larger estimation error components in (4.14) resulting into reduced performance. The simulation is done for first set of RBs after pilot-based initial estimation. As the block time index (t^b) increases,

the estimation accuracy measured by α_e increases which results into even better performance in steady state.

The higher mobility scenario needs a smaller number of symbols in an RB (T). Figure 4.10 compares the proposed algorithm with pilot-based estimation for its SEP versus SNR performance with varying T. The estimation error components in proposed algorithm depend on T as shown in (4.18). Therefore, reducing T amplifies the error components resulting into reduced performance. There is one favorable effect of reduced T, i.e., the sharp fall in SEP with SNR. This sharp fall is caused by the dominance of error component $\Delta\mathbf{H}_A$ which does not have a direct dependence on SNR. This component reduces effectively and quickly with iterations of algorithm. Therefore, as soon as the SNR value is obtained within the supported boundary, the algorithm shows its ability to minimize SEP.

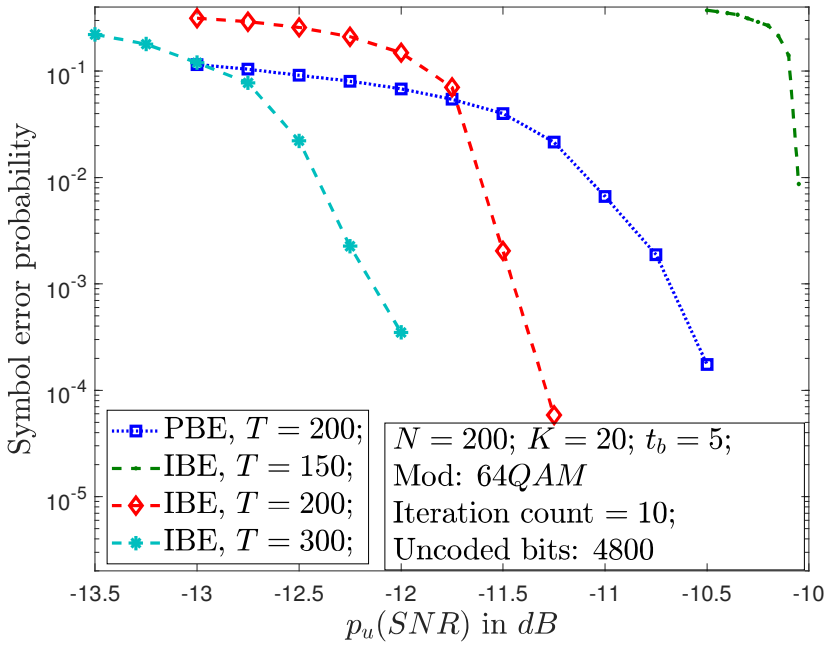

Figure 4.10. : Symbol error probability versus p_u (SNR) for different values of T with $K = 20$, $N = 200$, $\alpha_b = 0.8$ and $t^b = 5$. Capacity limited performance: same as in Figure 4.8.

The proposed scheme works under the combined effects of different system parameters which makes it powerful against the ill-conditioning of one parameter. The performance can be maintained by adjusting the controllable parameters to compensate an ill conditioned uncontrollable parameter. This approach makes the proposed algorithm robust against the scenario of higher mobility (i.e. lower coherence time or smaller T) where this case can be handled up to an extent by adjusting C_{max}, N, K, and p_u as shown in different SEP versus SNR plots. There are other mobile networking based techniques to deal with higher mobility where the processing at MTs is also considered which is however, beyond the scope of proposed scheme. The opportunistic communication is a good candidate for such cases as advocated in the literature for mobile networks [Liu *et al.*, 2016b; Zirwas, 2015; Liu *et al.*, 2014].

In this chapter, a blind channel estimation and tracking scheme is presented for massive MIMO systems by exploiting the temporal correlation in the channel and the error correction capability of turbo code. An insightful study of convergence and estimation error for the algorithm was presented. The simulation study revealed an improvement in the performance by the

proposed scheme over pilot-based channel estimation for a range of system parameters supporting a practical N/K value (≈ 10). The ranges of different system parameters (N, K, T, p_u, and α_b) are identified for the required performance of the system. The complexity analysis revealed the lower complexity of proposed algorithm than that of EVD and ILSP based similar schemes. After exploring the small scale fading channel matrix ($\mathbf{H}$) in this chapter, the large scale fading plus path loss matrix ($\mathbf{D}$) will be exploited in next chapter for an improvement in the system.

...